Acta Cryst. (1954). **7**, 385

A Statistical Structure for Crystalline Rubber

BY S. C. NYBURG

Department of Chemistry, University College of North Staffordshire, Keele, Staffordshire, England

(*Received* 1 *February* 1954)

There are stereochemical anomalies in the crystal structure of rubber put forward by Bunn. The crystal structure has been re-examined at liquid-air temperature using a technique analogous to single-crystal analysis. It is shown that these stereochemical anomalies can be removed by assuming a statistical crystal structure wherein a given molecule or its mirror image in $y = \frac{1}{8}$ is equally likely. Quantitative intensity estimates have been made and resulting structure-factor agreement is improved markedly over that for the structure proposed by Bunn.

1. Introduction

It has long been known that when sufficiently extended, natural rubber partially crystallizes and gives good X-ray fibre diagrams (Katz, 1925*a*, *b*). If wide sheets of rubber are highly stretched, not only is there preferred crystallite orientation parallel to the direction of stretch but also in the plane of the sheet ('higher orientation'; Mark & v. Susich, 1928).

There have been several attempts to solve the crystal structure (Meyer, 1950). The fibre axis of 8·1–8·2 Å implies a molecular chain with the carbon atoms of the 'backbone' *cis* to the double bonds (I). Further, the molecule cannot be planar but must have a staggered form.

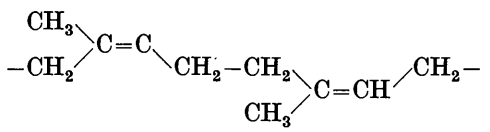

(I)

The most detailed analysis is due to Bunn (1942), who utilized 'higher orientation' to index the reflexions and estimated their intensities qualitatively. The structure proposed was based on a unit cell containing four molecules, each composed of two isoprene, C_5H_8, units. Adjacent C_5H_8 units were said to be somewhat different in configuration and each was characterized by a marked bending of the methyl groups out of the $-CH_2-\dot{C}=CH-CH_2-$ planes.

Although the broad features of the crystal structure have been accepted, in view of the high energy to be anticipated for these distortions, serious doubts have been expressed concerning the molecular configuration (Jeffrey & Orr, 1942). Similar distortions were invoked by Bunn to account for the crystal structures of the closely related β-gutta percha (*trans*-polyisoprene) and polychloroprene (*trans*-poly-2-chlorobutadiene) and were thought to account for some of the physical characteristics of the polymers. Criticisms of these bond distortions received added weight when Jeffrey (1944) showed that X-ray intensities calculated for a β-gutta-percha structure involving no distortions gave as good qualitative agreement with experimental values as did the structure proposed by Bunn. To date, there have been no attempts to put these analyses on a quantitative footing in order to assess the various proposals with more certainty.

2. Experimental

The preferred orientation obtained in wide stretched sheets can be characterised by angular distributions $\bar{\varphi}$, $\bar{\varphi}'$, and $\bar{\gamma}$ about the three principal axes of strain

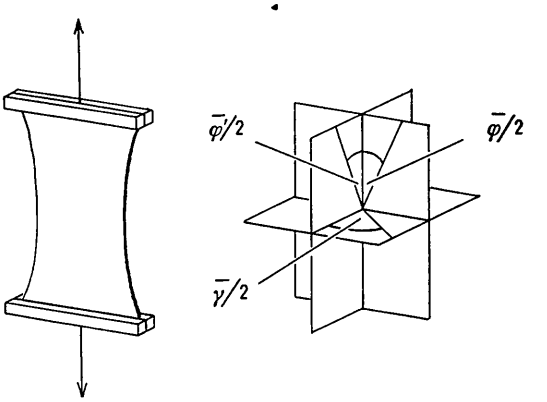

Fig. 1. Preferred orientation about principal axes of strain.

(Fig. 1). These distributions are defined from the spread of reflexion intensity in the appropriate plane by

$$\bar{\varphi} = \int_{-180°}^{+180°} I d\varphi / I_{\max.}, \text{ etc.}$$

Such a deformation does not necessarily give the best over-all resolution of reflexions for analytical purposes but the dependence of preferred orientation on strain is not fully known (Nyburg, 1954).

The necessity for a wide sheet handicaps quantitative intensity measurements because of variable absorption, especially at glancing angles to the beam; the presence of stretching clamps also hinders the recording of

reflexions. Both these objections were overcome as follows. The rubber, in the form of a sheet about 60×30×3 mm., was stretched almost to breaking point by clamps securing the 60 mm. edges. It was then placed in a container maintained at −25° C., at which temperature it crystallized further and hardened to such an extent that after 2–3 days the clamps could be removed without retraction occurring. From this sheet small narrow lengths, parallel to the direction of stretch were cut with a sharp edge. These specimens were mounted vertically on a single-crystal goniometer having a liquid-air cooling attachment similar to that described by Lonsdale (1941).

Nickel-filtered copper radiation was used throughout. Six separate multiple-film photographs were taken with the normal to the plane of the sheet making (acute) angles of $7\frac{1}{2}°$, $22\frac{1}{2}°$, $37\frac{1}{2}°$, $52\frac{1}{2}°$, $67\frac{1}{2}°$, $82\frac{1}{2}°$ to the plane of the incident beam. After some exposures the specimens were curved slightly (owing presumably to uneven cooling) and were replaced by new ones. In addition to these 'higher orientation' photographs, four multiple-film exposures were made, under identical conditions, with narrow specimens, simply extended. Two of these had the specimen vertical and merely differed in exposure time to give a large intensity range; the other two were tilted to record meridional reflexions. Such photographs are analogous to single-crystal rotation photographs and are referred to below as 'rotation' photographs to distinguish them from 'higher orientation' photographs.

Intensity estimations

For structure analysis, integrated intensities are required, but, because of disorientation of crystallites, accurate photometry is prohibitively onerous. It is simpler, and for our present purpose sufficient, to estimate plateau intensities at reflexion centres, by eye, against a calibrated set of intensities. Correction for disorientation is applied later.

The six 'higher orientation' photographs were used for indexing and the 'rotation' photographs for intensity estimation. Exposure factors and orientation $\bar{\gamma}$ for 'higher orientation' photographs are *a priori* unknown, but by trial and error it is possible to assign a set of exposure factors such that a *self-consistent* preferred orientation applies to all reflexions on both the right- and left-hand sides of all six photographs. The result of intensity estimations and applied corrections for the [201+$\bar{2}$01] reflexion (unit cell given below) is illustrated in Fig. 2. Graphical integration gives the value of $\bar{\gamma}$ as 77°.

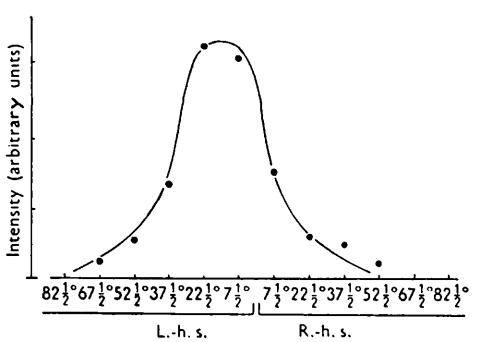

Fig. 2. Preferred orientation $\bar{\gamma}$ for the [201+$\bar{2}$01] reflexion using self-consistent exposure factors.

Orientations $\bar{\varphi}$ and $\bar{\varphi}'$ were obtained by photometry after correction for finite beam width (Nyburg, 1954). The value obtained for both $\bar{\varphi}$ and $\bar{\varphi}'$ was 8·5°.

Correction of measured intensities

Corrections have to be considered for the following factors:

(i) *Disorientation of crystallites.*—The intensity contours of three reflexions at the same ϱ (= 2 sin θ) in reciprocal space are illustrated in Fig. 3, in which the fibre axis is vertical. The upper reflexion is meridional, the lower equatorial and the other, general, reflexion subtends an angle δ at the equator. Since $\bar{\varphi} = \bar{\varphi}'$ the meridional reflexion is a circular spherical cap in R-space. The effective 'longitudinal' orientation for the general reflexion round the fibre axis is given by $(\bar{\varphi}+\bar{\omega})$, where

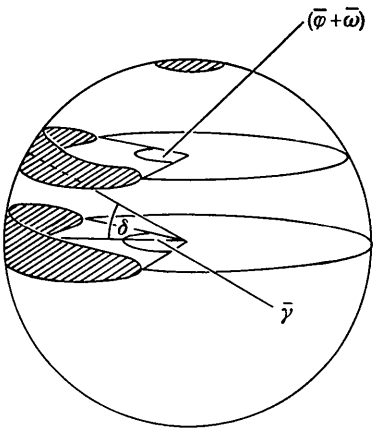

Fig. 3. R-space intensity contours of three reflexions.

$$\bar{\omega} = (\bar{\gamma}-\bar{\varphi}) \cos \delta \quad \text{and} \quad \delta = \tan^{-1}\zeta/\xi ,$$

ξ, ζ being R-space co-ordinates of the general reflexion centre. The intensity of the reflexion maxima in R-space is inversely proportional to the contour volume for a given structure factor. Since $\bar{\varphi}$ is small and the diffraction width is constant (see (iv) below), the contour volume is approximately proportional to $\bar{\varphi}(\bar{\varphi}+\bar{\omega})$. Hence reflexions with equal ϱ have to be multiplied by $(\bar{\varphi}+\bar{\omega})$. To allow for ϱ it is simplest to regard the arcs as derived from a powder photograph with preferred orientation. The intensities are corrected for varying ϱ with the standard powder photograph correction. For cylindrical cameras at other than equatorial points the required correction is complicated in form, but for reflexions restricted to comparatively

small θ values, the normal $\cos\theta/\sin 2\theta$ correction is adequate. The errors involved are small and are partially compensated by errors caused by disregarding finite beam width (see (iii) below).

(ii) *Polarization of reflected radiation.*—This is allowed for by multiplication by the usual $(1+\cos^2 2\theta)$ factor.

(iii) *Length of arc.*—The lengths of arcs on the photographs are not related by the geometry of the R-space contours alone since the finite width of the incident beam lengthens the shorter ones (small θ) to a greater extent than the longer ones. The effect is small and was neglected in view of its compensating effect on errors in (i).

(iv) *Diffraction width of the reflexions.*—Since the diffraction width (radial broadening) of the reflexions appeared constant and small throughout, the usual Lorentz $1/\sin 2\theta$ correction was applied for oblique intersection of reflexion contours with the reflexion sphere.

(v) *Film-incidence factor.*—The factor, P, used was Whittaker's (1953) modification of that due to Cox & Shaw.

(vi) *Absorption.*—No correction was made for absorption. It does however probably play a significant role in the discrepancy between observed and calculated structure factors since the specimens had to be cut as strips 1–1·5 mm. wide to overcome the tendency of narrower strips to curl up.

The complete form of the corrections applied to measured intensities was thus

$$I_{\text{corr.}} = I_o \frac{\sin^2\theta\cos\theta}{(1+\cos^2 2\theta)}(\bar{\varphi}+\bar{\omega})P\,.$$

Values of $\sin^2\theta\cos\theta/(1+\cos^2 2\theta)$ were taken from published values (Henry, Lipson & Wooster, 1951).

Indexing of reflexions

The unit cell proposed by Bunn was monoclinic with

$$a = 12{\cdot}46,\ b = 8{\cdot}89,\ c = 8{\cdot}1\ \text{Å (fibre axis)},\quad \beta = 92°.$$

Space group: $P2_1/a$

General positions:

'Down' molecules: (x, y, z) and $(\frac{1}{2}+x, \frac{1}{2}-y, z)$.
'Up' molecules: $(-x, -y, -z)$ and $(\frac{1}{2}-x, \frac{1}{2}+y, -z)$.

This unit cell is almost identical with one proposed earlier by Morss (1938), and with its assignment it is the x and z axes which tend to lie preferentially in the plane of the extended sheet. The β angle of 92° was preferred by Bunn on the basis of the failure of $[402+\bar{4}02]+[322+\bar{3}22]$ to fall exactly where required by a (pseudo)orthorhombic cell. The difference, however, is small. For $\beta = 90°$, $\varrho_{402} = \varrho_{\bar{4}02} = 0{\cdot}62$, whereas for $\beta = 92°$, $\varrho_{402} = 0{\cdot}63$ and $\varrho_{\bar{4}02} = 0{\cdot}61$. No resolution of 402 and $\bar{4}02$ was noted in the present work and $[322+\bar{3}22]$ is definitely absent. No inconsistencies were found using a unit cell with the above translations and a β angle of 90°. A more refined technique would be required to establish the value of β with more precision. The effect on the structure analysis is, in any case, extremely slight.

3. Structure analysis

It is clear from the broad qualitative agreement between observed and calculated intensities that the crystal structure proposed by Bunn is correct in outline. There is little doubt that the molecules in z projection are centred approximately on $x = \frac{1}{4}$, $y = \frac{1}{8}$, and the symmetry repeats $(\frac{1}{4}, \frac{5}{8})$, $(\frac{3}{4}, \frac{3}{8})$, $(\frac{3}{4}, \frac{7}{8})$. Molecular distortions were introduced primarily to account for intensities of the $hk0$ zone. This feature of the trial analysis was fully confirmed; despite extensive trials, no co-ordinates of conventional molecules could be established which fitted the experimental data as well as did the distorted molecule.

The number of observed $hk0$ reflexions is remarkably low (see Table 3) and appears to be confined first, when $h+k$ is even, to those for which $h = 2n$ and $k = 4n$, and secondly, when $h+k$ is odd, to those for which $h = 2n+1$ and $k = 2$. If the space group is $P2_1/a$ the z-projected electron density is of the form

$$\sum_{h+k=2n}\sum F(hk0)\cos 2\pi hx\cos 2\pi ky - \sum_{h+k=2n+1}\sum F(hk0)\sin 2\pi hx\sin 2\pi ky\,,$$

and it follows that these absences demand, at the point $x = \frac{1}{4}$, $y = \frac{1}{8}$ (and related points), symmetry planes parallel to $x = 0$ and to $y = 0$.

This feature underlines the structural peculiarities, since no conventional polyisoprene molecule can possess two planes of symmetry in projection along its length *unless it is planar*. As pointed out, the planar molecule is eliminated by the 8·1 Å fibre axis.

Evidence for a statistical structure

Because of the structural peculiarities, one is driven to consider the possibility of statistical arrangements of molecules. We concentrate attention first on the question as to whether a suitable statistical combination of conventional molecules will improve the structure-factor agreement in $hk0$ projection over that proposed by Bunn. We defer the question as to what actual structures are possible until later. Since the suggestion, due to Bunn, that adjacent isoprene groups in a chain have different bond lengths and angles is intuitively difficult to accept and does not appear warranted by the experimental evidence (see § 4), the molecule used for trial analysis had adjacent isoprene groups identical and invoked conventional bond lengths and angles only. This gives one plane of symmetry in z projection. Placing this symmetry plane on $x = \frac{1}{4}$, the atomic co-ordinates were found which gave

the best structure-factor agreement for such a molecule *plus* its mirror image in $y = \frac{1}{8}$ (to give the additional plane of symmetry). Fig. 4 shows z projections

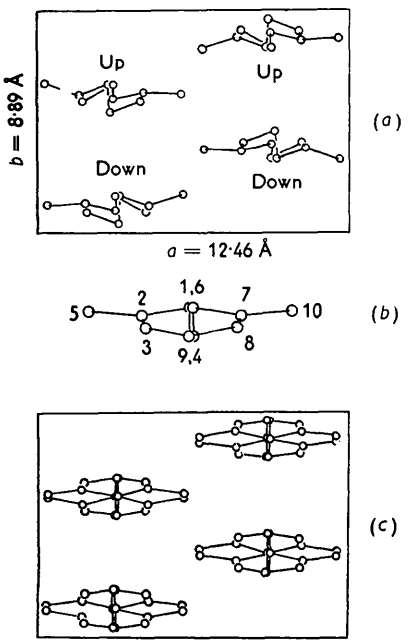

Fig. 4. Projections along z axis of (*a*) structure due to Bunn, (*b*) proposed isolated molecule, (*c*) proposed structure.

for (*a*) the structure due to Bunn, (*b*) the single molecule used for trial analysis, and (*c*) the combined 'statistical molecules' having atomic co-ordinates giving the best fit with the experimental data. These co-ordinates improved the $F(hk0)$ discrepancy from 0·49 (Bunn) to 0·21. (Details of structure-factor calculations are given in § 4.)

Possible statistical structures

There are only two types of feasible statistical structure giving the required symmetry in z projection: (i) that in which 'up' and 'down' molecules are arranged at random; (ii) that which has, for any atom in a molecule lying closest to the line $x = \frac{1}{4}$, $y = \frac{1}{8}$, an equally probable atom mirrored in the $y = \frac{1}{8}$ plane (and similarly mirrored atoms for the other three related molecules).

Examination of $h0l$ intensities revealed that no statistical structure of type (i) could be postulated to agree with observed intensities. Structure (ii), on the other hand, leaves $F(h0l)$ unaffected, necessitating examination of $0kl$ intensities. The $0kl$ zone shows only the reflexions 040 and 004 which can be unambiguously indexed. Using y co-ordinates derived from the z projection and z co-ordinates compatible with normal bond lengths and angles, only these reflexions are predicted to be observable. The structure due to Bunn, on the other hand, implies that six further $0kl$ reflexions should be observed. This was taken as confirmatory that the structure is statistical of type (ii). Further confirmatory evidence is provided by the greatly improved over-all structure-factor agreement (§ 5).

Detailed description of the structure

The best structure-factor agreement on the $hk0$ and $0kl$ zones was sufficient to fix all the atomic co-ordinates. The fractional atomic co-ordinates for two mirror-related molecules lying nearest the line $x = \frac{1}{4}$, $y = \frac{1}{8}$ are given in Table 1. Mirroring in the plane $y = \frac{1}{8}$ is evidenced by the sum of alternative y co-ordinates being $\frac{1}{4}$ throughout.

A single molecule is illustrated in Fig. 5(*a*). To avoid confusion, bond lengths only are shown on the lower

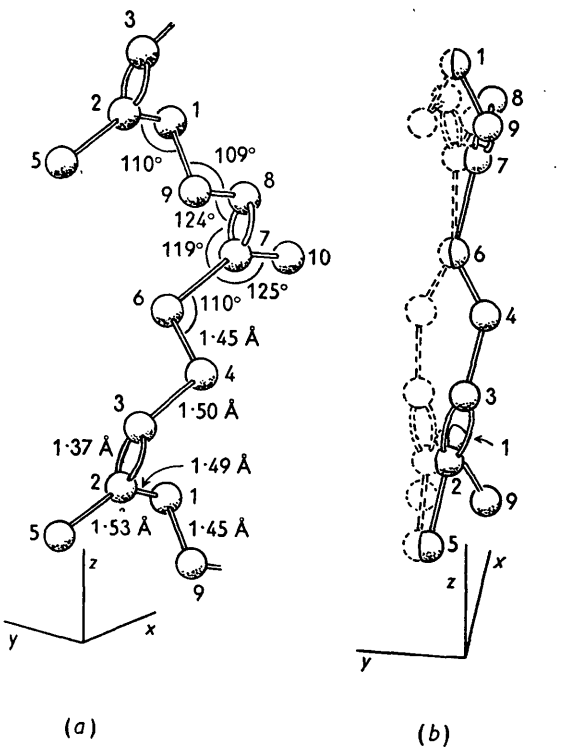

Fig. 5. (*a*) Isolated molecule. (*b*) Mirror-related pair of molecules.

Table 1. *Fractional atomic co-ordinates for mirror-related molecules lying on* $x = \frac{1}{4}$, $y = \frac{1}{8}$

	C_1	C_2	C_3	C_4	C_5	C_6	C_7	C_8	C_9	C_{10}
x	0·247	0·145	0·151	0·255	0·032	0·253	0·355	0·349	0·245	0·468
y	0·123	0·099	0·063	0·039	0·113	0·123	0·099	0·063	0·039	0·113
	0·127	0·151	0·187	0·211	0·137	0·127	0·151	0·187	0·211	0·137
z	0·213	0·306	0·471	0·560	0·235	0·713	0·806	0·971	0·060	0·735

isoprene group and angles only on the upper group; the two groups are identical in configuration. The parameters are very similar to those established in the crystal-structure analysis of the *trans*-di-isoprene compound geranylamine hydrochloride (Jeffrey, 1945). As in that structure, the isoprene groups are planar and are connected by slightly short bonds* having normal tetrahedral angles between them. A different view of the molecule, together with its mirror-related form, is illustrated in Fig. 5(*b*). The planarity of the isoprene groups C_1 to C_5 and of C_6 to C_{10} (C_{10} is hidden) is clearly seen.

The postulation of a statistical structure of this type raises two subsidiary questions. First, whether adjacent chains along the y axis (the chains are staggered along the x axis and there are no special interactions caused by the proposed mirroring) are mirrored at random about the y planes on which they are centred. Secondly, whether isoprene groups in a *given* chain are mirrored at random.

When a molecular chain is mirrored, it does not 'fit' the structure quite so well as previously: it either lies slightly too close to, or too far from, its immediate neighbour. This effect is shown in the x projections of Fig. 6(*a*) and (*b*); in both cases there is a change of 'sense' of mirroring at X. The effect, which is comparatively small, may be due to errors in co-ordinates. Further refinement may remove it. If it does occur, the smaller separation (Fig. 6(*b*)) invokes closest inter-

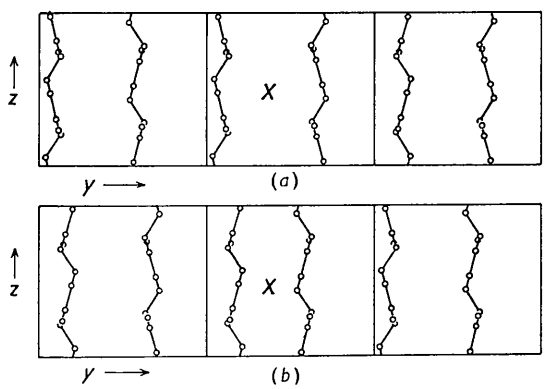

Fig. 6. Changes in 'sense' of mirroring causing (*a*) increase in distance between neighbouring molecules, (*b*) decrease between neighbouring molecules.

molecular carbon separations of about 3·1 Å. This is smaller than the accepted values (3·5–4·0 Å). Nevertheless, a slight redistribution of intermolecular spacings would overcome the localized interaction and cause a minor 'fault' in the structure.

A definite negative answer can be given as to whether isoprene groups in given chains are mirrored at random. Simple mirroring cannot occur, for the bond angles produced are quite unfeasible. The y co-ordinates can be modified to give a feasible molecule exhibiting a change in sense along its length, but this is definitely ruled out by too close a proximity to neighbouring molecules.

* *Note added in proof*, 8 *April* 1954.—It now appears that the shortening of these bonds is not significant (Cruickshank, private communication).

4. Comparison of observed and calculated structure factors

Calculated structure factors

All the atoms in the proposed structure have co-ordinates related to those of atoms C_1 to C_5. For $P2_1/a$ the structure factor is easily shown to be:

(i) $h+k = 2n$

$$F(hkl) = 4\sum_{i=1}^{5} f_i[\{\cos 2\pi ky + \cos \tfrac{1}{2}k\pi \cos 2\pi ky + \sin \tfrac{1}{2}k\pi \sin 2\pi ky\} \times \{\cos 2\pi(hx+lz) + \cos \pi(h+l) \cos 2\pi(hx-lz)\}];$$

thus, in addition to the usual absences, $F(hk0) = 0$ for k odd; further $F(hkl) = F(\bar{h}kl)$.

(ii) $h+k = 2n+1$

$$F(hkl) = -4\sum_{i=1}^{5} f_i[\{\sin 2\pi ky + \sin \tfrac{1}{2}k\pi \cos 2\pi ky - \cos \tfrac{1}{2}k\pi \sin 2\pi ky\} \times \{\sin 2\pi(hx+lz) - \cos \pi(h+l) \sin 2\pi(hx-lz)\}];$$

whence $F(hk0) = 0$ for k odd and $F(hkl) = -F(\bar{h}kl)$.

Atomic scattering factors f_i were those of McWeeny (1951) for carbon valence states. No allowance was made for scattering by hydrogen. Because of the approximations used by Bunn the structure factors for his case were recalculated. Terms hx, etc. were calculated to three figures; trigonometric functions were of two-figure accuracy.

Observed structure factors

Crystallites having x axes pointing in opposite directions are present to equal extents in any specimen so that, since β lies close to 90°, reflexions hkl from half the crystallites fall in the same place as reflexions $\bar{h}kl$ from the other half. For Bunn's crystal structure $F(hkl) \neq F(\bar{h}kl)$ so that the observed intensity must be considered as derived from an effective structure factor $F'(hkl)$, where

$$F'(hkl) = \{\tfrac{1}{2}[F^2(hkl)+F^2(\bar{h}kl)]\}^{\frac{1}{2}}.$$

Terms $F(hkl)$, $F(\bar{h}kl)$ and resultant $F'(hkl)$ are given in Table 3.

For the new structure $F(hkl) = \pm F(\bar{h}kl)$, so that $F'(hkl)$ need not be calculated. The sign given in the table is for $F(hkl)$; the sign of $F(\bar{h}kl)$ is the same if $h+k = 2n$, but changed if $h+k = 2n+1$.

In some cases several reflexions overlap in R-space and give rise to an intensity contour in which individual

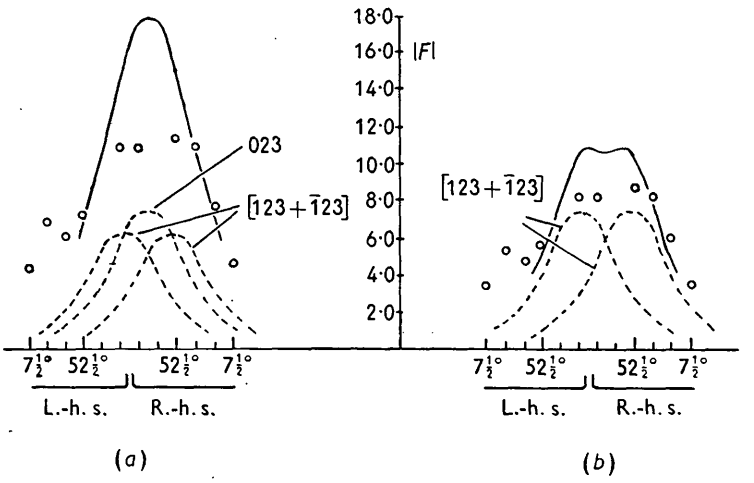

Fig. 7. $|F_c|$ values for unresolved 023 and [123+1̄23] reflexions for (*a*) the structure due to Bunn, (*b*) the present structure. Curves for individual reflexions derived from Fig. 2 by taking square roots of ordinates. Points are corrected F_o values (scaled to $\Sigma F_o = \Sigma|F_c|$) obtained from 'higher orientation' photographs and used for indexing purposes only.

reflexions may, or may not, be still resolvable. In either case the predicted form of the contour is determined graphically from the calculated structure factors, the known angular separation of reflexions and the form of $\bar{\gamma}$. An example is taken from Table 3. The 023 reflexion has $\xi = 0{\cdot}35$ and the [123+1̄23] reflexion has $\xi = 0{\cdot}37$. These lie too close in R-space to be resolved, and only a single peak is derived when data from successive 'higher orientation' photographs are plotted. To compare the data of Bunn on an equal footing ΣF_o has to be equated to $\Sigma|F_c|$ for both structures. The data are compared in Table 2 and illustrated in Fig. 7.

Table 2

	Bunn	Nyburg
Intensity of observed peak on 'rotation' photographs with		
$\Sigma F_o = \Sigma\|F_c\|$	13·1	9·8
F (023)	7·5	0·0
F'(123)	6·4	7·4
Graphically calculated peak	18·0	11·0

The general reflexion [*hkl*+$\bar{h}$*kl*] has a weight of 4 on 'rotation' photographs from which intensity values are obtained; the multiplicity for index triples involving zero is easily derived. Where overlapping occurs care has to be exercised in deriving the correct multiplicity. In the above example the combined peak has multiplicity 2 so that 'rotation' intensities are halved. (The multiplicity for an individual [123+1̄23] reflexion is 4 but the peak calculation includes this combination twice.)

Because of disorientation, the minimum detectable $F'(hkl)$ increases with ϱ. Unlike the case of single-crystal analysis, direct comparisons of F_o with F_c for all ϱ prejudice the over-all agreement since at higher ϱ values even quite high F_c values do not give rise to observable intensities. From the smallest observed intensity the minimum observable value of $F'(hkl)$ for all ϱ is derived (Fig. 8). It is doubtful if increased exposure would improve this greatly because of back-

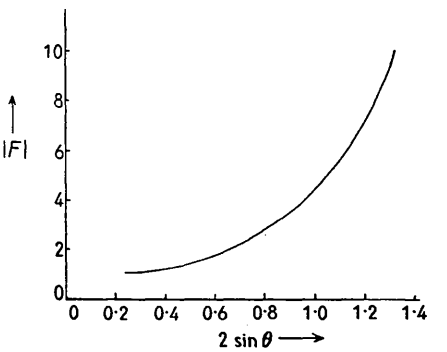

Fig. 8. Minimum detectable $|F|$ values.

ground scatter. F_c values which fall below this curve are bracketed in Table 3 and counted as zero for the discrepancy calculation.

Table 3. *Structure-factor table*

F_c(B) are for structure due to Bunn; F_c(N) are for this structure. F_o scaled to $\Sigma F_o = \Sigma|F_c(\mathrm{N})|$; to scale for F_c(B) multiply F_o by 1·33. (F_c with brackets count zero.)

Equator

2 sin θ	*hkl*	F_c(B)	F_c(N)	F_o
0·21	110	(+1·5)	(0·0)	—
0·25	200	−30·3	−28·7	28·7
0·30	210	(0·0)	(0·0)	—
0·35	020	+2·0	(0·0)	—
0·37	120	−42·9	−38·4	39·0
0·41	310	(+1·6)	(0·0)	—
0·43	220	−5·1	(0·0)	—
0·49	400	+11·0	+9·8	22·5
0·51	320	+4·9	+3·2	—
0·52	410	(+0·7)	(0·0)	—
0·53	130	(+0·9)	(0·0)	—
0·58	230	(−0·9)	(0·0)	—
0·60	420	−2·3	(0·0)	—

Table 3 (*cont.*)

2 sin θ	*hkl*	F_c(B)	F_c(N)	F_o
0·64	330	(+1·6)	(0·0)	—
0·64	510	(0·0)	(0·0)	—
0·69	040	−22·1	−16·0	21·2
0·70	140	(−1·5)	(0·0)	—
0·71	520	−3·2	−4·4	6·9
0·72	430	−2·4	(0·0)	—
0·74	240	+3·6	(−1·5)	—
0·74	600	(+0·2)	(−0·5)	—
0·76	610	(+0·5)	(0·0)	—
0·79	340	(+0·3)	(0·0)	—
0·81	530	(+0·5)	(0·0)	—
0·82	620	(−2·5)	(0·0)	—
0·85	440	(+1·6)	−2·4	—
0·87	150	−3·9	(0·0)	—
0·88	710	(+0·6)	(0·0)	—
0·90	250	(+1·0)	(0·0)	—
0·91	630	(−2·3)	(0·0)	—
0·93	540	+6·4	(0·0)	—
0·93	720	(+0·3)	(+0·8)	—
0·94	350	(−3·8)	(0·0)	—
0·99	800	+14·2	+16·1	15·7
1·00	450	(−1·0)	(0·0)	—
1·01	730	(−1·2)	(0·0)	—
1·01	810	(+0·6)	(0·0)	—
1·04	060	(+2·3)	(0·0)	—
1·05	160	+5·9	(+0·4)	—
1·05	820	(+0·5)	(0·0)	—
1·06	550	(−2·1)	(0·0)	—
1·07	260	(+0·8)	(0·0)	—
1·07	640	−5·4	(−2·6)	—
1·10	360	(+4·6)	(+2·8)	—
1·11	740	(−0·3)	(0·0)	—
1·12	830	(−2·1)	(0·0)	—
1·13	910	(+0·3)	(0·0)	—
1·14	650	(+0·1)	(0·0)	—
1·15	460	+7·1	(0·0)	—
1·17	920	−20·0	−19·9	14·7
1·21	840	(−5·6)	(−4·5)	—
1·21	560	(−6·2)	(+4·8)	—
1·22	170	(+1·4)	(0·0)	—
1·22	750	(+0·1)	(0·0)	—
1·23	930	(−0·7)	(0·0)	—
1·24	10,0,0	−21·6	−22·4	17·4
1·24	270	(+1·1)	(0·0)	—
1·25	10,1,0	(0·0)	(0·0)	—
1·27	370	(+0·3)	(0·0)	—
1·28	660	(−4·7)	(0·0)	—

1st layer line

2 sin θ	*hkl*	F_c(B)		F_c(N)		F_o
0·19	001	−2·9		(0·0)		—
0·26	011	+2·6		(0·0)		—
0·29	{111 / 1̄11}	−7·2 / −6·2	6·7	+8·0		3·9
0·31	{201 / 2̄01}	−23·5 / +25·6	24·5	−22·5		26·2
0·36	{211 / 2̄11}	+7·6 / +7·1	7·4	−10·3		3·7
0·40	021	−5·7		0·0		
0·41	{121 / 1̄21}	−20·9 / +17·5	22·4	−18·8	18·8	19·5
0·45	{311 / 3̄11}	+9·6 / +9·4	9·5	+11·1		7·3
0·47	{221 / 2̄21}	+5·8 / +4·3	5·1	−1·6		—
0·50	{401 / 4̄01}	+1·1 / −0·8	1·4	(−0·3)		—

Table 3 (*cont.*)

2 sin θ	*hkl*	F_c(B)		F_c(N)		F_o
0·54	{321 / 3̄21}	+5·9 / −2·8	4·6	(+0·8)		—
0·55	031	−5·5		(0·0)		—
0·56	{411 / 4̄11}	−2·6 / −5·0	4·0	+3·2		—
0·57	{131 / 1̄31}	0·0 / +2·1	(1·5)	+1·9		—
0·61	{231 / 2̄31}	+7·9 / +8·1	8·0	+3·5		6·7
0·63	{421 / 4̄21}	−2·1 / −5·3	4·0	(−0·5)		—
0·67	{331 / 3̄31}	−2·7 / −3·2	3·0	−3·7		5·9
0·67	{511 / 5̄11}	−1·0 / +1·9	(1·5)	(−0·1)		—
0·72	041	−3·8		(0·0)		—
0·73	{141 / 1̄41}	+6·3 / +0·7	4·5			—
0·74	{521 / 5̄21 / 431 / 4̄31}	−8·2 / +2·1 / −9·6 / −0·7	9·1	−3·7 / −2·0	3·0	1·7
0·76	{241 / 2̄41}	+12·7 / −6·2	10·0	+7·7		6·4
0·76	{601 / 6̄01}	−1·8 / +2·6	4·5	−2·4	4·8	3·4
0·79	{611 / 6̄11}	−4·5 / −4·0		−6·3		
0·81	{341 / 3̄41}	−1·1 / −6·6	4·7	(0·0)		—
0·83	{531 / 5̄31}	−2·7 / +0·9	(2·0)	(−2·5)		—
0·84	{621 / 6̄21}	+5·0 / −8·5	7·0	(+1·3)		—
0·87	{441 / 4̄41}	−5·0 / −2·4	(3·9)	(+1·6)		—
0·89	051	(−0·9)		(0·0)		—
0·90	{151 / 1̄51}	+8·3 / −0·4	5·9	(−0·5)		—
0·90	{711 / 7̄11}	−6·8 / −6·3	6·5	−6·0		4·7
0·92	{251 / 2̄51}	+0·7 / −0·6	(0·6)	(+0·5)		—
0·93	{631 / 6̄31}	−1·9 / −5·0	(3·8)	(−2·3)		—
0·95	{541 / 5̄41}	+4·5 / +1·7	(3·4)	(0·0)		—
0·95	{721 / 7̄21}	−6·3 / +7·2	6·8	−9·5		5·1
0·96	{351 / 3̄51}	−8·9 / −4·7	7·2	(−0·1)		—
1·00	{801 / 8̄01}	−9·2 / +10·1	9·6	−10·3		7·7
1·02	{451 / 4̄51}	−1·2 / +1·6	(1·4)	(+0·2)		—
1·03	{731 / 7̄31}	+2·8 / +3·0	(2·9)	(+2·8)		—

2nd layer line

2 sin θ	*hkl*	F_c(B)		F_c(N)		F_o
0·64	032	+2·2		(+0·5)		—
0·65	{412 / 4̄12}	−10·7 / +10·6	10·7	−10·8		11·2

Table 3 (*cont.*)

2 sin θ	*hkl*	F_c(B)		F_c(N)		F_o
0·66	{132 / $\bar{1}$32}	−0·5 / −2·4	(1·8)	(−1·7)		—
0·69	{232 / $\bar{2}$32}	+1·2 / −0·2	(1·2)	(+0·6)		—
0·71	{422 / $\bar{4}$22}	+0·5 / +0·6	(0·6)	(0·0)		—
0·74	{332 / $\bar{3}$32}	−3·8 / +3·5	3·7	(−1·7)		—
0·75	{512 / $\bar{5}$12}	−12·2 / +10·3	11·3	−10·4		16·0
0·79	042	+9·2		+19·1		
0·80	{522 / $\bar{5}$22}	+4·3 / +4·7		+9·0		
0·80	{142 / $\bar{1}$42}	−5·5 / −3·2	13·0	0·0	21·2	26·0
0·81	{432 / $\bar{4}$32}	−6·3 / +9·7		−6·2		
0·83	{242 / $\bar{2}$42}	+1·3 / +0·9	(1·1)	−3·6		—
0·83	{602 / $\bar{6}$02}	−2·2 / −2·1	7·9	+0·4	7·6	6·0
0·85	{612 / $\bar{6}$12}	+6·6 / −8·5		+7·6		

3rd layer line

2 sin θ	*hkl*	F_c(B)		F_c(N)		F_o
0·60	013	(−1·1)		(0·0)		—
0·61	{113 / $\bar{1}$13}	+1·9 / −5·3	4·0	(−1·2)		6·0
0·62	{203 / $\bar{2}$03}	+0·5 / −4·3	3·0	+2·4		—
0·65	{213 / $\bar{2}$13}	+1·9 / −3·3	2·7	(+0·1)		—
0·67	023	−7·5		0·0		
0·68	{123 / $\bar{1}$23}	+4·4 / −8·0	18·0	+7·4	11·0	9·8
0·70	{313 / $\bar{3}$13}	−3·9 / +2·1	3·1	(−1·3)		—
0·71	{223 / $\bar{2}$23}	+2·8 / +8·9	6·6	(0·0)		—
0·76	{403 / $\bar{4}$03}	+7·4 / −5·3		+5·6		
0·77	{323 / $\bar{3}$23}	+7·2 / −3·2	10·6	+4·7	9·0	12·4
0·78	{413 / $\bar{4}$13}	+1·2 / +1·5		+0·7		

4th layer line

2 sin θ	*hkl*	F_c(B)	F_c(N)	F_o
0·76	004	+16·0	+17·0	17·0

The case of 001 is of interest. This reflexion is at its maximum when the plane of the extended sheet is tilted 5·5° from the vertical. There is lack of agreement concerning its detection. Bunn (1942) and Sauter (1937) report it present but faint. Morss, on the other hand, did not detect it. It could not be detected in the present case. A radial diffuse streak was always present in the vicinity of the 001 position but no genuine reflexion. F(001) at its maximum, for Bunn's crystal structure, should be considerably stronger than 'faint': with $\varrho = 0{\cdot}19$, $F_c = -2{\cdot}9$, twice the minimum observable. The absence of 001 was taken as indicating identity of configuration of adjacent isoprene groups in a chain.

F_o values in Table 3 are adjusted to give $\Sigma F_o = \Sigma|F_c|$ for the new structure. To compare the data of Bunn, F_o values should be multiplied by 1·33.

5. Discussion

The discrepancy, $\Sigma||F_o|-|F_c|| \div \Sigma F_o$, for the structure proposed by Bunn is 0·58 compared with the value of 0·31 for the structure proposed here. This is a marked improvement and must be considered satisfactory in view of the errors necessarily involved in converting arc plateau intensities to F_o values.

A refinement of atomic co-ordinates would improve the agreement, but probably the sources of greatest error lie in absorption and intensity correction approximations.

The new type of structure envisaged here for rubber may apply equally well to the related cases of β-gutta-percha and chloroprene to which, at present, the same objections concerning the proposed molecular configuration are applicable.

I am grateful to Dr D. P. Elias for taking a tilted-specimen photograph to establish the magnitude of the 004 reflexion. This work arose out of a programme of research initiated by the Board of the British Rubber Producers' Research Association.

References

Bunn, C. W. (1942). *Proc. Roy. Soc.* A, **180**, 40.
Henry, N. F. M., Lipson, H. & Wooster, W. A. (1951). *The Interpretation of X-Ray Diffraction Photographs*, p. 246. London: Macmillan.
Jeffrey, G. A. (1944). *Trans. Faraday Soc.* **40**, 517.
Jeffrey, G. A. (1945). *Proc. Roy. Soc.* A, **183**, 388.
Jeffrey, G. A. & Orr, W. J. C. (1942). *Trans. Faraday Soc.* **38**, 382.
Katz, J. R. (1925*a*). *Chemiker-ztg.* **49**, 353.
Katz, J. R. (1925*b*). *Naturwissenschaften*, **13**, 410.
Lonsdale, K. (1941). *J. Sci. Instrum.* **18**, 133.
McWeeny, R. (1951). *Acta Cryst.* **4**, 813.
Mark, H. & Susich, G. v. (1928). *Kolloidzschr.* **46**, 11.
Meyer, K. H. (1950). *Natural and Synthetic High Polymers*, 2nd ed., vol. 4, pp. 188 *et seq.* New York: Interscience Publishers.
Morss, H. A. (1938). *J. Amer. Chem. Soc.* **60**, 237.
Nyburg, S. C. (1954). *Brit. J. Appl. Phys.* In the press.
Sauter, E. (1937). *Z. phys. Chem.* B, **36**, 405.
Whittaker, E. J. W. (1953). *Acta Cryst.* **6**, 218.